Acriflavine inhibits HIF-1 dimerization, tumor growth, and vascularization

KangAe Lee[a,b], Huafeng Zhang[a,c], David Z. Qian[a,c], Sergio Rey[a,b], Jun O. Liu[c,d], and Gregg L. Semenza[a,b,c,e,1]

[a]Vascular Program, Institute for Cell Engineering, [b]McKusick–Nathans Institute of Genetic Medicine, Departments of [c]Oncology, [d]Pharmacology, and [e]Pediatrics, Medicine, Radiation Oncology, and Biological Chemistry, The Johns Hopkins University School of Medicine, Baltimore, MD 21205

Contributed by Gregg L. Semenza, August 18, 2009 (sent for review July 17, 2009)

HIF-1 is a heterodimeric transcription factor that mediates adaptive responses to hypoxia and plays critical roles in cancer progression. Using a cell-based screening assay we have identified acriflavine as a drug that binds directly to HIF-1α and HIF-2α and inhibits HIF-1 dimerization and transcriptional activity. Pretreatment of mice bearing prostate cancer xenografts with acriflavine prevented tumor growth and treatment of mice bearing established tumors resulted in growth arrest. Acriflavine treatment inhibited intratumoral expression of angiogenic cytokines, mobilization of angiogenic cells into peripheral blood, and tumor vascularization. These results provide proof of principle that small molecules can inhibit dimerization of HIF-1 and have potent inhibitory effects on tumor growth and vascularization.

cancer | chemotherapy | hypoxia | xenograft

Solid tumors frequently contain hypoxic regions because they have high rates of cell proliferation and form aberrant blood vessels (1). Intratumoral hypoxia is associated with increased risk of invasion, metastasis, and patient mortality (2). The adaptation of cancer cells to hypoxia is critical for their survival. Hypoxia-inducible factor 1 (HIF-1) activates transcription of genes encoding proteins that mediate major adaptive responses to hypoxia (2). For example, HIF-1 activates the expression of vascular endothelial growth factor (VEGF), a key regulator of angiogenesis, as well as glucose transporters (e.g., GLUT1) and glycolytic enzymes (e.g., hexokinase [HK] 1 and 2), which are required for high levels of glucose uptake and metabolism (2). The fact that HIF-1 regulates the expression of multiple gene products involved in tumor metabolism and vascularization suggests that a greater anticancer effect may be achieved by inhibition of HIF-1, as compared to a downstream gene product, such as VEGF.

HIF-1 is a heterodimeric protein that is composed of HIF-1α and HIF-1β subunits, which belong to the family of basic helix–loop–helix (bHLH) transcription factors that contain a PER-ARNT-SIM (PAS) domain (3). In contrast to the constitutively expressed HIF-1β subunit, high levels of HIF-1α are induced in response to hypoxia. HIF-1α is constantly synthesized and, in well-oxygenated cells, is hydroxylated on proline residue 402 and/or 564, which is required for binding of the von Hippel-Lindau protein, the recognition subunit of an E3 ubiquitin ligase that targets HIF-1α for proteasomal degradation (4). Asparagine 803 is also hydroxylated, which inhibits recruitment of the coactivator proteins p300 and CREB binding protein (CBP) to the transcriptional activation domain of HIF-1α. The prolyl and asparaginyl hydroxylases require O_2 for their catalytic activity. Under hypoxic conditions, hydroxylation decreases, HIF-1α accumulates and dimerizes with HIF-1β to form a functional transcription factor capable of DNA binding at hypoxia response elements (HREs) and transcriptional activation. HIF-2α is another bHLH-PAS protein that is O_2-regulated, dimerizes with HIF-1β, and binds to HREs (4).

Increased HIF-1α or HIF-2α levels are found in human lung, colon, breast, and prostate carcinomas, and are associated with disease progression and increased patient mortality (2). A large body of experimental data indicates that disruption of HIF-1 signaling inhibits tumor growth in mouse models (2). A growing number of drugs have been identified that (*i*) inhibit HIF-1 activity through a reduction in HIF-1 mRNA or protein levels, HIF-1 DNA binding, or transactivation of target genes; and (*ii*) have anticancer activity in preclinical studies (5). However, no drugs have been identified that bind directly to HIF-1.

Dimerization of HIF-1β with HIF-1α or HIF-2α, which is required for HIF-1 DNA binding and transcriptional activity, is mediated by bHLH and PAS domains located in the amino-terminal half of each subunit (3, 6). A small molecule that targets HIF-1 dimerization might function as a selective HIF-1 inhibitor, but current pharmacological dogma holds that small molecules are unlikely to disrupt large dimerization interfaces, such as the combined HLH and PAS domains, which span over 200 amino acids (aa). In this study, we identified an inhibitor of HIF-1 dimerization, which decreased HIF-1 transcriptional activity and showed anticancer efficacy in vivo that was due at least in part to its antiangiogenic effects.

Results

Screening for Inhibitors of HIF-1 Dimerization. We developed a cell-based dimerization assay based on complementation of split *Renilla* luciferase (*R*luc) (7). In this case, dimerization of the HIF-1α and HIF-1β bHLH-PAS domains provided the mechanism for complementation (Fig. 1*A*). Interaction of HIF-1$\alpha_{12–396}$ and HIF-1$\beta_{11–510}$ causes the N- and C-terminal halves of *R*luc to be closely approximated, thereby reconstituting *R*Luc activity. Vectors encoding N*R*Luc-HIF-1$\alpha_{12–396}$ and HIF-1$\beta_{11–510}$-C*R*Luc fusion proteins were cotransfected with control reporter pGL2-promoter, in which firefly luciferase (*F*luc) coding sequences are downstream of an SV40 promoter. *R*luc activity was detected in cells expressing N*R*Luc-HIF-1$\alpha_{12–396}$ and HIF-1$\beta_{11–510}$-C*R*Luc, but no *R*luc activity was observed when either N*R*Luc-HIF-1$\alpha_{12–396}$ or HIF-1$\beta_{11–510}$-C*R*Luc was expressed alone (Fig. 1*B*).

To validate the specificity of the split *R*luc assay, we coexpressed N*R*Luc-HIF-1$\beta_{11–510}$ and found that it competes with HIF-1$\beta_{11–510}$-C*R*Luc for binding to N*R*Luc-HIF-1$\alpha_{12–396}$, and thereby blocks reconstitution of *R*luc activity (*SI Appendix*, Fig. S1*A*). We also coexpressed a double-mutant form of HIF-1α (HIF-1α_{DM}) that contains Pro-to-Ala substitutions at residues 402 and 564, thereby preventing hydroxylation and rendering HIF-1α stable under nonhypoxic conditions. HIF-1α_{DM} competed with N*R*Luc-HIF-1$\alpha_{12–396}$ for dimerization with HIF-1$\beta_{11–510}$-C*R*Luc (*SI Appendix*, Fig. S1*B*). The finding that increasing concentrations of N*R*Luc-HIF-1$\beta_{11–510}$ or HIF-1α_{DM} led to decreasing *R*luc activity confirmed that *R*luc activity was dependent on N*R*Luc-HIF-1$\alpha_{12–396}$::HIF-1$\beta_{11–510}$-C*R*Luc interaction and indicated that the assay was suitable for identifying inhibitors of HIF-1 dimerization.

Author contributions: K.L., D.Z.Q., and G.L.S. designed research; K.L., H.Z., D.Z.Q., and S.R. performed research; J.O.L. contributed new reagents/analytic tools; K.L., H.Z., D.Z.Q., S.R., and G.L.S. analyzed data; and K.L. and G.L.S. wrote the paper.

The authors declare no conflict of interest.

[1]To whom correspondence should be addressed. E-mail: gsemenza@jhmi.edu.

This article contains supporting information online at www.pnas.org/cgi/content/full/0909353106/DCSupplemental.

www.pnas.org/cgi/doi/10.1073/pnas.0909353106

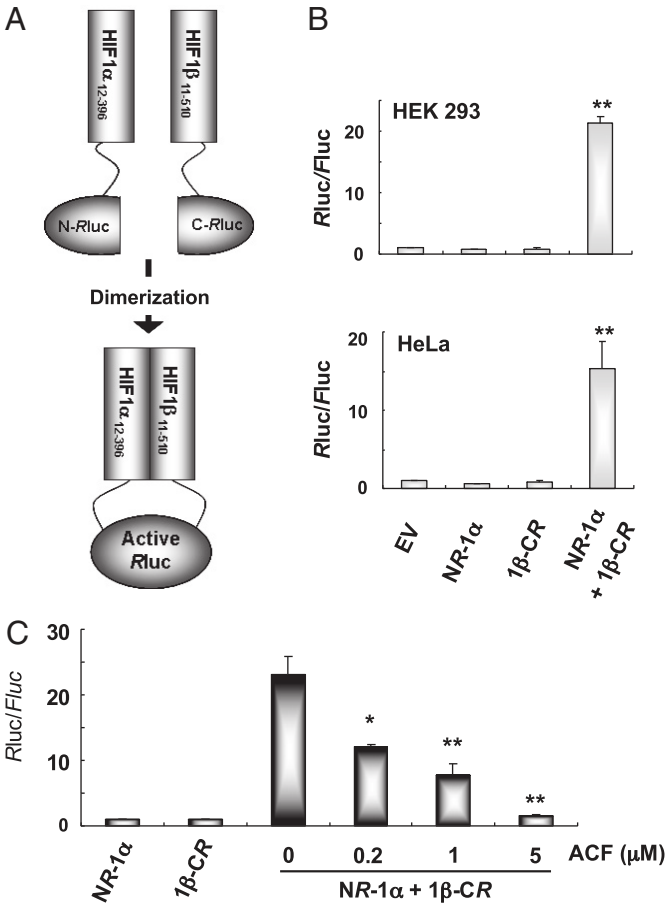

Fig. 1. Split *R*luc system for identifying inhibitors of HIF-1 dimerization. (*A*) N-terminal and C-terminal portions of *R*luc were attached to HIF-1α_{12-396} and HIF-1β_{11-510}, respectively. (*B*) The ratio of *Renilla*/firefly luciferase activity (*R*luc/*F*luc) was determined using cells co-transfected with pGL2-promoter, which encodes *F*luc, and N*R*luc-HIF-1α_{12-396} (N*R*-1α) and/or HIF-1β_{11-510}-C*R*luc (1β-C*R*). Each value was normalized to the results for empty vector (EV). Data represent mean ± SEM ($n = 6$). **, $P < 0.01$ (Student's *t* test) vs. EV. *C*, HEK293 cells were cotransfected with pGL2-promoter, N*R*-1α, and 1β-C*R* vectors and treated with acriflavine (ACF) for 24 h. The *R*luc/*F*luc ratio in cell lysates was determined and normalized to the results for N*R*-1α. Mean ± SEM are shown ($n = 6$). *, $P < 0.05$; **, $P < 0.01$ vs. 0 μM ACF (Student's *t* test).

We previously screened a collection of 3,120 drugs that are approved by the FDA or have entered phase II clinical trials and identified 336 drugs that inhibited hypoxia-induced transcription of HIF-1-dependent reporter plasmid p2.1 by >50% at a concentration of 10 μM (8). The top 200 hits were subjected to secondary screening using the split *R*luc assay. The most potent inhibitor of HIF-1 dimerization was acriflavine (ACF), which inhibited *R*luc activity by 94% at a concentration of 5 μM (Fig. 1*C*). ACF inhibited *R*luc in a dose-dependent manner with an IC_{50} of approximately 1 μM.

Acriflavine Inhibits the Dimerization of HIF-1α (or HIF-2α) with HIF-1β. To confirm that ACF inhibits dimerization of HIF-1α and HIF-1β, we performed coimmunoprecipitation (co-IP) assays. HEK293 cells were treated with ACF or vehicle and exposed to 20 or 1% O_2 for 24 h. IP with anti-HIF-1α antibodies (Ab) showed that ACF decreased interaction between endogenous HIF-1α and HIF-1β in hypoxic cells (Fig. 2*A*). We also incubated a purified GST-HIF-1β_{11-510} fusion protein with lysates from cells transfected with Flag-HIF-1α_{DM} (Fig. 2*B*). Flag-HIF-1α_{DM} was pulled down with GST-HIF-1β_{11-510}, but not with GST alone, and the interaction was decreased when cells were treated with ACF. ACF also decreased the interaction between HIF-2α and endogenous HIF-1β (*SI Appendix*, Fig. S2*A*) or purified GST-HIF-1β_{11-510} (*SI Appendix*, Fig. S2*B*).

An in vitro binding assay was also performed using purified GST-HIF-1β_{11-510} and His-HIF-1α_{12-395} (or His-HIF-2α_{3-351}) proteins. His-HIF-1α_{12-395} (Fig. 2*C*) or His-HIF-2α_{3-351} (*SI Appendix*, Fig. S2*C*) was pulled down by GST-HIF-1β_{11-510}, but not by GST alone, and these interactions were inhibited by ACF. The ability of ACF to disrupt HIF-1 (Fig. 2*D*) or HIF-2 (*SI Appendix*, Fig. S2*D*) dimerization was dependent on the concentration of ACF. The observed IC_{50} was approximately 1 μM and 5 μM led to almost complete inhibition.

Acriflavine Binds Directly to HIF-1α and HIF-2α. To determine whether ACF binds to HIF-1β, purified GST-HIF-1β_{11-510} was preincubated with ACF and the complex was captured by glutathione beads, washed 1–3 times to eliminate unbound ACF, and then incubated with purified His-HIF-1α_{12-395}. Preincubation of GST-HIF-1β_{11-510} with ACF did not inhibit dimerization of GST-HIF-1β_{11-510} and His-HIF-1α_{12-395} when the preincubated complex was washed extensively (Fig. 3*A*; ×2 and ×3 wash). Moreover, His-HIF-1α_{12-395} levels captured by GST-HIF-1β_{11-510} did not decrease with increasing concentration of ACF during preincubation (Fig. 3*B*). These results indicate that HIF-1β is not a target of ACF. Next, purified His-HIF-1α_{12-395} was preincubated with ACF, captured by Ni-NTA-agarose beads, washed, and incubated with GST-HIF-1β_{11-510}. Preincubation of His-HIF-1α_{12-395} with ACF decreased binding of GST-HIF-1β_{11-510} even after extensive washing (Fig. 3*C*). This effect was dependent on the ACF concentration during preincubation (Fig. 3*D*). These results indicate that ACF binds to HIF-1α and disrupts its interaction with HIF-1β.

To confirm these conclusions, we determined the direct binding affinity of ACF to HIF-1α or HIF-2α by following the innate fluorescence of ACF at λ_{ex} = 463 nm and λ_{em} = 490 nm (*SI Appendix*, Fig. S3). Purified GST-HIF-1α_{3-350} or GST-HIF-2α_{3-351} was incubated with 0–250 μM ACF and captured by glutathione agarose beads. The protein-drug complex was washed 3 times and analyzed for fluorescence intensity (FI; Fig. 3*E*). The FI of GST-HIF-1α_{3-350} or GST-HIF-2α_{3-351} increased in a dose dependent manner as ACF concentration increased, whereas neither GST nor GST-HIF-1β_{11-510} showed increased FI even at high ACF concentrations. A significant difference between HIF-α subunits and control proteins was first observed at 1 μM ACF (Fig. 3*E Inset*) and FI was maximal at 100 μM.

Acriflavine Specifically Binds to PAS-B Subdomain of HIF-1α and HIF-2α. We tested purified proteins that contained different domains of HIF-1α for ACF binding (Fig. 4*A* and *SI Appendix*, Fig. S4 *A* and *B*). ACF increased the FI of all GST fusion proteins that contained the PAS-B domain, whereas no difference in FI was observed after ACF vs. vehicle treatment of all fusion proteins that lacked PAS-B. Maximal FI was captured by GST-HIF-1$\alpha_{235-350}$, which contained only PAS-B, whereas FI was not captured by GST-HIF-1α_{90-155}, which contained only PAS-A. Similar results were also observed for HIF-2α (Fig. 4*B* and *SI Appendix*, Fig. S4 *C* and *D*). For both HIF-1α and HIF-2α, a significant difference in captured FI between fusion proteins that included vs. excluded PAS-B was first observed at a concentration of 1 μM ACF (*SI Appendix*, Fig. S4 *B* and *D Inset*). These results indicate that ACF interacts specifically with the PAS-B subdomain of HIF-1α or HIF-2α.

The aryl hydrocarbon receptor (AHR) is a bHLH-PAS transcription factor that also heterodimerizes with HIF-1β. The binding of ACF to GST-fusion proteins containing AHR residues 1–410 (bHLH-PAS) or 281–410 (PAS-B) was not significantly different from GST alone (*SI Appendix*, Fig. S5), indicating that ACF does not bind to AHR. To test whether ACF blocks heterodimerization

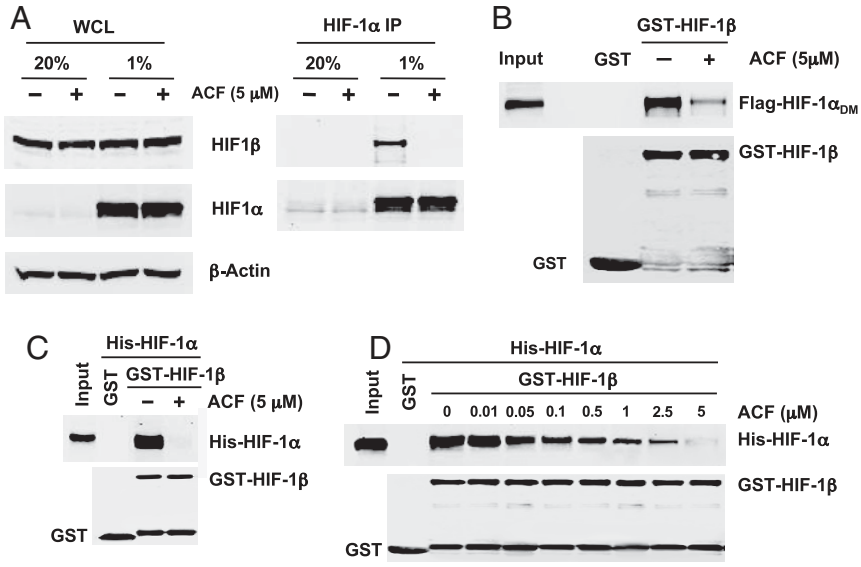

Fig. 2. Inhibition of HIF-1 dimerization by ACF. (*A*) Effect of ACF on HIF-1α:HIF-1β interaction was determined using coimmunoprecipitation (co-IP). HEK293 cells were treated with ACF or vehicle and exposed to 20 or 1% O_2 for 24 h. IP of whole cell lysates (WCL) was performed with anti-HIF-1α antibodies (Ab). WCL and IP products were assayed by immunoblot (IB) to detect HIF-1β, HIF-1α, and β-actin. (*B*) GST-HIF-1$\beta_{11–510}$ was incubated with WCL from HEK293 cells transfected with vector encoding Flag-HIF-1α_{DM} in the presence or absence of ACF. Proteins were pulled down with glutathione-Sepharose-4B beads and subjected to IB assays using anti-FLAG and anti-GST Ab. An aliquot of WCL was analyzed directly by IB assay (Input). (*C*) Purified His-HIF-1$\alpha_{12–395}$ was incubated with purified GST-HIF-1$\beta_{11–510}$ or GST in the presence of ACF or vehicle overnight at 4 °C. Binding was determined by GST pull down and IB using anti-His and anti-GST Ab. An aliquot of His-fusion protein was analyzed directly by IB assay (Input). (*D*) Dose-dependent effects of ACF on HIF-1 dimerization in vitro were determined.

by inducing HIF-1α homodimerization, purified GST-HIF-1$\alpha_{3–350}$ or GST-HIF-1$\beta_{11–510}$ was incubated with lysates obtained from HEK293 cells exposed to 1% O_2 in the presence of ACF or vehicle. HIF-1α was captured by GST-HIF-1$\beta_{11–510}$ and ACF decreased the interaction between HIF-1α and GST-HIF-1$\beta_{11–510}$, whereas no HIF-1α was captured by GST-HIF-1$\alpha_{2–350}$ in the presence of ACF (*SI Appendix*, Fig. S6*A*). His-HIF-1$\alpha_{12–395}$ also failed to capture GST-HIF-1$\alpha_{3–350}$ in the presence of ACF (*SI Appendix*, Fig. S6 *B* and *C*). Thus, ACF does not induce homodimerization of HIF-1α.

Acriflavine Inhibits HIF-1 DNA Binding and Transcriptional Activity. To investigate the functional consequences of disrupting HIF-1 dimerization, we first determined the effect of ACF on the binding of endogenous HIF-1 to DNA in living cells. Chromatin-bound HIF-1α was immunoprecipitated from HEK293 cells after exposure to 20% or 1% O_2 in the presence of 0–10 μM ACF. HIF-1 binding sites from the *VEGF* and *PDK1* genes were specifically amplified by PCR from chromatin that was immunoprecipitated from cells exposed to 1% O_2 but not from chromatin that was immunoprecipitated from cells exposed to 20% O_2, demonstrating hypoxia-induced binding of HIF-1 in the absence of drug (Fig. 5*A*). Treatment of hypoxic cells with ACF inhibited binding of HIF-1α to DNA in a dose dependent manner. ACF also blocked binding of HIF-2α to the *VEGF* and *PDK1* genes in hypoxic cells (*SI Appendix*, Fig. S7). We next determined the effect of ACF on HIF-1 transcriptional activity. HEK293 cells were cotransfected with HIF-1-dependent *F*luc reporter p2.1 and pSV-Renilla, and exposed to 20% or 1% O_2. ACF significantly inhibited the hypoxic induction of *F*luc activity in a dose dependent manner with an IC_{50} of approximately 1 μM and complete inhibition at 5 μM (Fig. 5*B*). Hypoxic induction of VEGF and GLUT1 mRNA was also blocked by ACF (Fig. 5*C*). ACF did not affect HIF-1α protein accumulation (Fig. 5*D*).

Acriflavine Does Not Affect HIF-1α:Hsp90 Interaction or MYC-mediated Transcription. HIF-1α interacts with the chaperone Hsp90 and disruption of HIF-1α:Hsp90 association leads to proteasomal degradation of HIF-1α (9). Similar levels of Hsp90 were coimmunoprecipitated with HIF-1α from lysates of hypoxic HEK293 cells treated with ACF or vehicle, indicating that ACF does not disrupt the interaction between HIF-1α and Hsp90 (*SI Appendix*, Fig. S8*A*). We also tested whether ACF affects MYC-mediated transcription using human P493 cells with tetracycline-repressible MYC activity (10). Expression of fibrillarin (FBL) and apurinic/apyrimidinic exonuclease (APEX) mRNAs, which are products of MYC target genes, was blocked by tetracycline (*SI Appendix*, Fig. S8*B*). ACF did not affect FBL or APEX mRNA levels, whereas ACF specifically decreased hypoxia-induced GLUT1 mRNA expression.

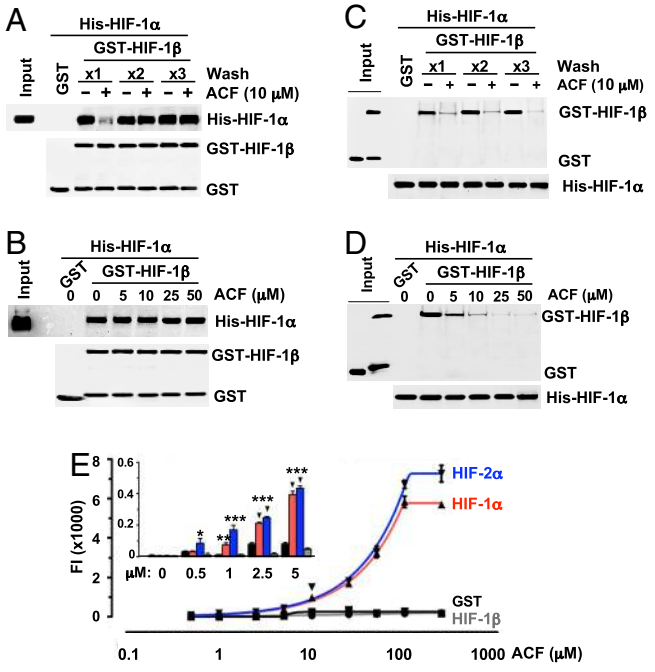

Fig. 3. ACF binds directly to HIF-1α and HIF-2α. (*A*) Purified GST-HIF-1$\beta_{11–510}$ was preincubated with vehicle (-) or ACF (+) and the complex was captured by glutathione beads, subjected to one to three washes, incubated with purified His-HIF-1$\alpha_{12–395}$, washed again, and proteins bound to glutathione were analyzed by IB using anti-His and anti-GST Ab. An aliquot of His-HIF-1$\alpha_{12–395}$ was analyzed directly by IB assay (Input). (*B*) Effect of preincubating GST-HIF-1$\beta_{11–510}$ with ACF was determined as described above. (*C*) His-HIF-1$\alpha_{12–395}$ was preincubated with ACF, captured by Ni-NTA agarose, subjected to one to three washes, and incubated with GST-HIF-1$\beta_{11–510}$. The proteins bound to Ni-NTA agarose were analyzed by IB using anti-His and anti-GST Ab. Aliquots of GST and GST-HIF-1$\beta_{11–510}$ were analyzed directly by IB assay (Input). (*D*) His-HIF-1$\alpha_{12–395}$ was preincubated with ACF and then incubated with GST-HIF-1$\beta_{11–510}$ and analyzed as described above. (*E*) GST fusion proteins were incubated with 0–250 μM ACF, captured by glutathione beads, washed, and analyzed for fluorescence intensity (FI; mean ± SEM; $n = 6$). FI analysis at low ACF concentrations is shown (*Inset*).

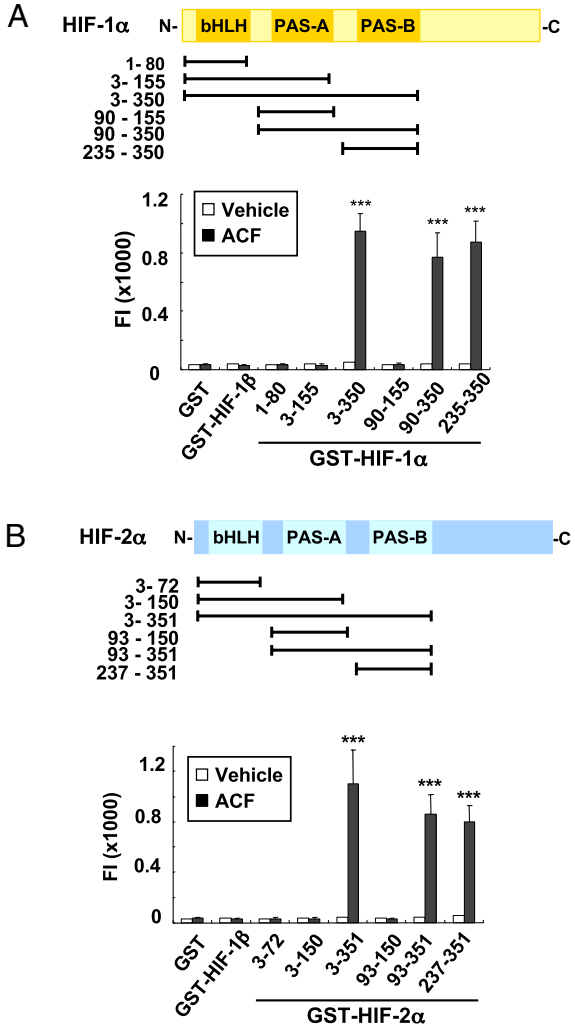

Fig. 4. ACF binds to the PAS-B domain of HIF-1α and HIF-2α. *(A)* GST-HIF-1α proteins were generated containing indicated HIF-1α residues (*Top*), incubated with ACF or vehicle, captured with glutathione beads, washed, and analyzed for fluorescence intensity (FI) (*Bottom*). Mean ± SEM are plotted ($n = 6$) ***, $P < 0.001$ vs. GST (two-way ANOVA with Bonferroni correction). *(B)* GST-HIF-2α proteins were generated containing indicated HIF-2α residues (*Top*). ACF binding was determined by FI (*Bottom*). Mean ± SEM is shown ($n = 3$). ***, $P < 0.001$ vs. GST (two-way ANOVA with Bonferroni correction).

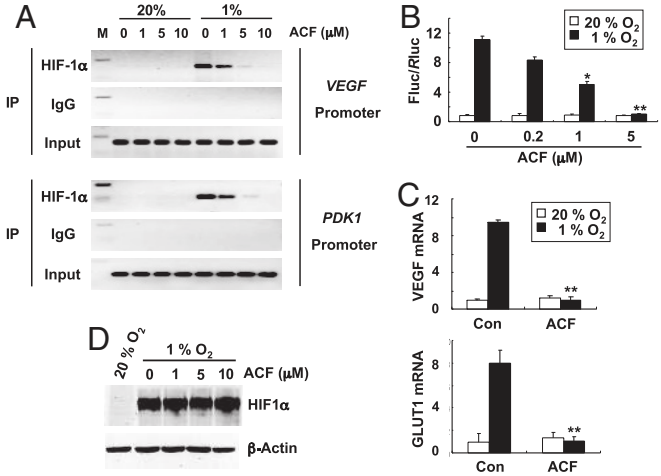

Fig. 5. ACF inhibits HIF-1 DNA-binding and transcriptional activity. *(A)* HEK293 cells were exposed to 20% or 1% O_2 and 0–10 μM ACF. Input DNA was isolated from an aliquot of lysate before IP. The remaining lysate was divided and incubated with anti-HIF-1α Ab or rabbit IgG for IP. PCR was performed using immunoprecipitates as template to amplify sequences from the *VEGF* and *PDK1* promoters, which contain known HIF-1 binding sites. PCR products were analyzed by gel electrophoresis and ethidium bromide staining. M, size marker. *(B)* Cells were cotransfected with reporter plasmid p2.1, in which transcription of *F*luc sequences was driven by an HRE upstream of an SV40 promoter, and reporter plasmid pSV-Renilla, in which *R*luc sequences were transcribed from the SV40 promoter. After 24-h incubation, cells were treated with ACF and exposed to 20% (white bar) or 1% (black bar) O_2 for 24 h. Cells were lysed and *F*luc/*R*luc ratio was determined (mean ± SEM; $n = 6$). *, $P < 0.05$; **, $P < 0.01$ (two-way ANOVA with Bonferroni correction). *(C)* Cells were exposed to 20% (white bar) or 1% (black bar) O_2 for 24 h in the presence of vehicle (Con) or 5 μM ACF. Total RNA was isolated for determination of VEGF and GLUT1 mRNA levels. HIF-1 target gene mRNA levels relative to 18S rRNA were calculated as $2^{-\Delta(\Delta Ct)}$ where $\Delta Ct = Ct_{target} - Ct_{18S}$ and $\Delta(\Delta Ct) = \Delta Ct_{control} - \Delta Ct_{treatment}$ where control = vehicle–treated cells at 20% O_2. Mean ± SEM is plotted ($n = 4$). **, $P < 0.01$ (two-way ANOVA with Bonferroni correction). *(D)* HIF-1α and β-actin protein levels were determined by IB assays of cells cultured at 20% or 1% O_2 in the presence of 0–10 μM ACF for 20 h.

Acriflavine Inhibits Tumor Xenograft Growth. We examined whether inhibition of HIF-1 dimerization by ACF affects the growth of human cancer xenografts. ACF did not affect HIF-1α or HIF-2α mRNA or protein levels in PC-3 human prostate cancer cells and Hep3B-c1 cells (*SI Appendix*, Figs. S9 and S10). ACF also did not affect the levels of HIF-1β, c-Myc, Hsp90, or β-Actin protein in PC-3 or Hep3B-c1 cells (*SI Appendix*, Fig. S10). These data rule out nonspecific effects of ACF on transcription or translation at concentrations that block HIF-1 activity. In contrast, HRE-dependent transcription (*SI Appendix*, Fig. S9*B*) and the expression of VEGF, stromal-derived factor 1 (SDF1), stem cell factor (SCF), and GLUT1 mRNAs, which are all encoded by HIF-1 target genes (*SI Appendix*, Fig. S9*C*), were significantly inhibited by treatment of PC-3 cells with ACF. ACF had no effect on PC-3, P493, or Hep3B-c1 cell cycling, proliferation, or survival at concentrations that block HIF-1 activity (*SI Appendix*, Fig. S11).

To investigate the effect of ACF on tumor growth, vehicle or ACF was administered by daily i.p. injection to severe combined immune deficiency (SCID) mice that received s.c. PC-3 cell xenografts. Treatment was initiated 3 days before implantation and continued for 32 days. Tumors were palpable in vehicle treated mice by day 12 and grew to approximately 500 mm^3 by day 32, whereas mice treated with ACF did not show any significant tumor growth even after one month (*SI Appendix*, Fig. S12). Daily administration of ACF did not cause weight loss (*SI Appendix*, Fig. S13*A*), suggesting ACF has no major systemic toxicity.

When treatment was delayed until 14 days after s.c. implantation of PC-3 cells, at which time the tumors had grown to approximately 100 mm^3, ACF inhibited tumor growth after 7 days of administration (days 14 through 21), which continued through day 28 (Fig. 6*A*) without any effect on body weight (*SI Appendix*, Fig. S13*B*). Expression of VEGF, SDF1, SCF, GLUT1, HK1, and HK2 mRNAs was decreased in tumors after treatment with ACF (Fig. 6*B*), whereas HIF-1α protein was highly expressed in tumors from mice treated with vehicle or ACF (*SI Appendix*, Fig. S14).

Next, Hep3B-c1 hepatoma cells stably transfected with the HIF-1-regulated *F*Luc reporter gene p2.1 were implanted in SCID mice. Before initiation of treatment (day 25), tumor volume (≈100 mm^3) was similar across groups (Fig. 6*C*). Analysis of HIF-1-dependent *F*Luc activity by whole-body Xenogen imaging revealed bioluminescence at the tumor site that was similar in both groups (Fig. 6*D Upper*). Mice were then treated with ACF or vehicle by daily i.p. injection and Xenogen imaging was repeated 4 h after treatment on day 28. The bioluminescence in tumors before and after treatment with vehicle was similar. In contrast, *F*Luc activity was markedly decreased after treatment with ACF for 4 days (Fig.

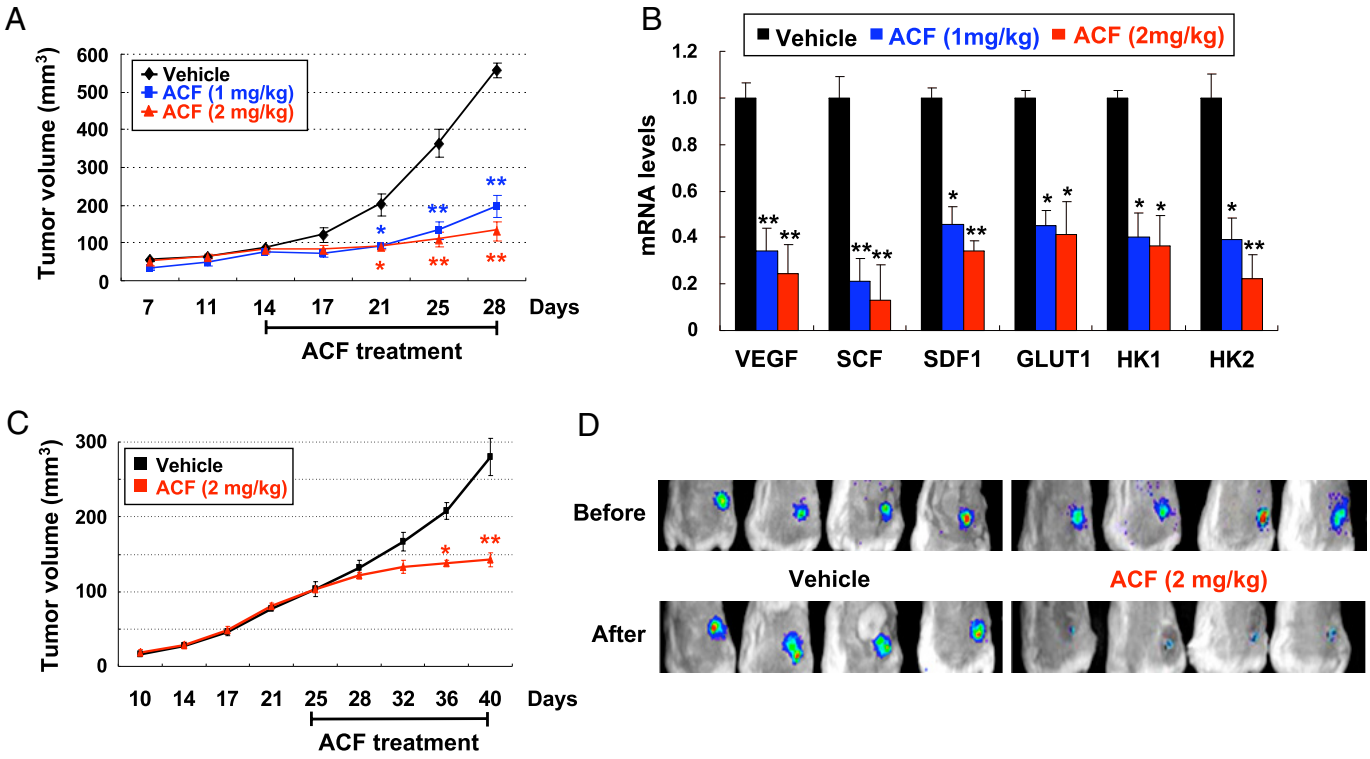

Fig. 6. ACF inhibits tumor growth, HIF-1 target gene expression, and HIF-1 activity. (*A* and *B*) PC-3 xenografts were grown to approximately 100 mm^3 and mice were treated by daily i.p. injection of vehicle or ACF for 14 days. (*A*) Tumor volume (mean ± SEM; $n = 4$) is shown. *, $P < 0.05$; **, $P < 0.01$ vs. vehicle (two-way ANOVA with Bonferroni correction). (*B*) Mice were euthanized on day 28 (4 h after last dose) and tumors were collected. mRNA levels relative to 18S rRNA in tumors from vehicle- and ACF-treated mice were calculated as $2^{-\Delta(\Delta Ct)}$, where $\Delta Ct = Ct_{target} - Ct_{18S}$ and $\Delta(\Delta Ct) = \Delta\, Ct_{vehicle} - \Delta Ct_{ACF}$. Mean ± SEM ($n = 4$) is shown. *, $P < 0.05$; **, $P < 0.01$ (two-way ANOVA with Bonferroni correction). (*C-D*) mice bearing Hep3B-c1 xenografts were treated with vehicle or ACF starting on day 25. (*D*) HRE-driven *F*Luc activity was determined by Xenogen imaging before treatment (*Upper*) and 4 h after treatment on day 28 (*Lower*).

6*D*, *Lower*), indicating that ACF inhibited HIF-1 activity in tumors, which preceded the significant inhibition of tumor growth that was first observed on day 36 (Fig. 6*C*). ACF administration for 15 days did not cause any loss of body weight (*SI Appendix*, Fig. S13*C*).

Acriflavine Inhibits Angiogenic Cell Mobilization and Tumor Vascularization. VEGF, SCF, and SDF1 induce the mobilization from bone marrow and other sites into peripheral blood of circulating angiogenic cells (CACs), a term that designates a heterogeneous population including endothelial progenitor, mesenchymal stem, myeloid, and other cell types that home to tumors and stimulate angiogenesis. HIF-1 plays a critical role in these processes (11). To determine the effect of ACF on CACs, SCID mice bearing PC-3 xenografts of approximately 50 mm^3 were treated with ACF for 9 days (*SI Appendix*, Fig. S15). Four hours after the last dose, blood was collected for flow cytometric analysis of CACs, as defined by the coexpression of a progenitor marker (CD34, CD117 [c-kit], or ScaI) and either VEGFR2 or CXCR4 (Fig. 7*A*). The number of $VEGFR2^+/CD117^+$, $VEGFR2^+/CD34^+$, and $CXCR4^+/ScaI^+$ CACs was increased approximately 5-fold in tumor-bearing mice compared with mice without tumors and no significant differences were observed between untreated and vehicle-treated tumor-bearing mice. In contrast, ACF treatment significantly decreased the number of CACs in tumor-bearing mice to levels observed in mice without tumors. ACF inhibited the expression of mRNAs encoding VEGF, SDF1, and SCF (which are the ligands bound by VEGFR2, CXCR4, and CD117, respectively) in PC-3 xenografts (Fig. 6*B*). SDF-1 protein levels were increased in blood from tumor-bearing vs. nontumor-bearing mice and ACF treatment for 9 days reduced SDF-1 in the blood of tumor-bearing mice to levels similar to those in nontumor bearing mice (Fig. 7*B*). These effects of ACF were associated with a significant reduction in tumor vascularization (Fig. 7*C*).

Discussion

There is interest in the discovery of drugs that target HIF-1 because of the critical role that it plays in cancer progression (1, 2, 5). Identifying an inhibitor of HIF-1 dimerization would be particularly desirable as a defined and selective mechanism of action, although conventional wisdom holds that the large interfaces involved in protein dimerization are difficult to disrupt by small molecules. We used a cell-based split-*R*luc assay to identify ACF as drug that inhibits HIF-1 dimerization (Figs. 1–3) by binding to the PAS-B subdomain of HIF-1α and HIF-2α (Fig. 4), thereby inhibiting HIF-1 DNA-binding and transcriptional activity (Figs. 5 and 6), leading to inhibition of tumor growth, CAC mobilization, and tumor vascularization (Figs. 6 and 7).

PAS domains of HIF-1α, HIF-2α, HIF-1β, and other bHLH-PAS proteins are organized into PAS-A and PAS-B subdomains, which contribute to dimerization by providing, in addition to the bHLH domain, secondary interaction surfaces that increase the specificity of dimerization. NMR spectrometry revealed that hydrophobic residues located on the solvent-exposed face of a β-sheet in the HIF-2α PAS-B subdomain mediate heterodimerization with HIF-1β (12). The HIF-2α PAS-B crystal structure was shown to contain an internal cavity, which accommodated a small molecule that partially disrupted the heterodimerization of isolated HIF-2α and HIF-1β PAS subdomains in vitro but was not reported to have any effect on heterodimerization of the full length proteins or on HIF-1 transcriptional activity (13). We show that ACF binds to the PAS-B subdomain of HIF-1α or HIF-2α, thereby blocking het-

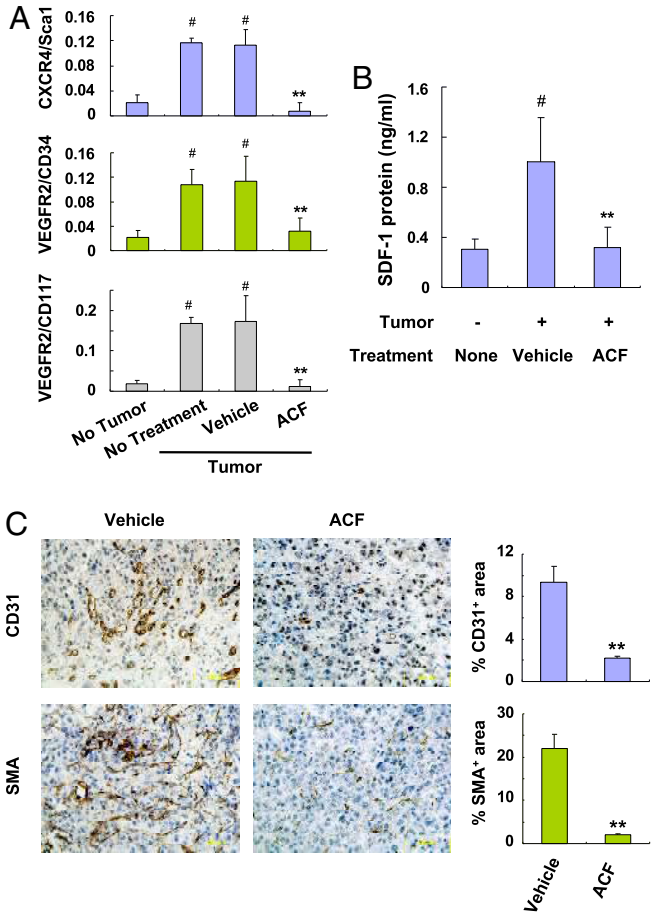

Fig. 7. ACF inhibits mobilization of angiogenic cells and tumor vascularization. Mice with approximately 100-mm^3 PC-3 xenografts were treated for 9 days with vehicle or 2 mg/kg/d ACF. Blood was collected 4 h after the last treatment and the percentage of mononuclear cells that were CXCR4$^+$/Scal$^+$, VEGFR2$^+$/CD34$^+$, or VEGFR2$^+$/CD117$^+$ (*A*) and serum levels of SDF-1 (*B*) were determined. Mean ± SEM shown ($n = 4$). #, $P < 0.01$ vs. non-tumor-bearing mice; **, $P < 0.01$ vs. vehicle-treated tumor-bearing mice (Student's *t* test). (*C*) Tumor sections were analyzed by immunohistochemistry (left panels) for CD31 and α-smooth muscle actin (SMA). The stained area in 20 fields was quantified (right panels). Mean ± SEM ($n = 4$ mice each) is shown. **, $P < 0.01$ (Student's *t* test).

erodimerization with HIF-1β and inhibiting HIF-1-dependent gene transcription in cultured cells and tumor xenografts.

ACF has known trypanocidal, antibacterial, and antiviral activities (14). Effects of ACF on cancer cells were first reported 50 years ago (15). In the present study, we have demonstrated that ACF administration inhibited the expression in prostate cancer xenografts of VEGF, SDF1, and SCF mRNA, which encode angiogenic cytokines that are critical for tumor vascularization through mobilization of CACs bearing the cognate receptors VEGFR2, CXCR4, and CD117, respectively. ACF treatment decreased tumor-induced CAC mobilization and vascularization, providing a mechanism for tumor growth arrest. ACF inhibited HIF-1 at concentrations that do not affect cell proliferation or survival ex vivo. However, the drug concentrations achieved in vivo were not determined and other mechanisms of action besides HIF-1 inhibition, such as NF-κB inhibition (16), may contribute to the anticancer effects of ACF.

ACF is a mixture of 3,6-diamino-10-methylacridinium chloride (trypaflavin) and 3,6-diaminoacridine (proflavine) (*SI Appendix*, Fig. S16). Our results provide proof-of-principle that small molecule inhibitors of HIF-1 dimerization in vivo can be identified. Unlike other drugs that indirectly inhibit HIF-1 activity, ACF binds directly to both HIF-1α and HIF-2α. ACF has been administered to patients for at least 5 months without major side effects (14), suggesting that it may be a candidate for clinical trials. ACF can also serve as the lead compound for development of drugs to treat patients with cancer subtypes in which increased HIF-1α or HIF-2α levels are associated with disease progression and patient mortality (2, 5).

Materials and Methods

Detailed materials and methods are available online in *SI Appendix*.

***Split Rluc* System.** DNAs encoding HIF-1α residues 12–396 and HIF-1β residues 11–510 were prepared by PCR (*SI Appendix*, Table S1) and cloned downstream of the *R*luc N-terminal region (residues 1–229) in pCMV-N*R*luc or upstream of the *R*luc C-terminal region (residues 230–311) in pCMV-C*R*luc, respectively (7). HEK293 and HeLa cells were cotransfected with 300 ng of N*R*luc-HIF-1$\alpha_{12–396}$, 300 ng of HIF-1$\beta_{11–510}$-C*R*luc, and 80 ng of pGL2-promoter, using Fugene-6 (Roche). After 7-h incubation, cells were treated with drug (9) or vehicle (0.1% DMSO) for 24 h.

Quantitative Real Time-Reverse Transcription-PCR Assay. Primers (*SI Appendix*, Table S2) were designed using Beacon Designer software (Bio-Rad).

Preparation of His-tagged and GST Fusion Proteins. HIF-1$\alpha_{12–395}$ and HIF-2$\alpha_{3–351}$ were amplified by using specific primers (*SI Appendix*, Table S3) and PCR products were cloned into pET-28c (Novagen). HIF-1β, HIF-1α, and HIF-2α residues were amplified using specific primers (*SI Appendix*, Table S4) and the PCR products were inserted into pGEX-5X-1 (GE Healthcare).

Chromatin IP (ChIP) Assay. The ChIP Assay Kit (Upstate-Cell Signaling Solution) was used with rabbit polyclonal anti-HIF-1α or HIF-2α Ab (Novus Biologicals) or rabbit IgG. *VEGF* and *PDK1* sequences were detected by PCR (*SI Appendix*, Table S5).

ACKNOWLEDGMENTS. We are grateful to S. Gambhir and P. Ramasamy (Stanford University), and K. Padgett (Novus Biologicals) for providing the split Renilla luciferase vectors and anti-HIF-2α Ab; G. Wang for assistance with assay development; J. Kim for assistance with fluorometry; K. Miyake for assistance with animal handling; K. Zeller and C. Dang for advice and reagents for assaying MYC; and M. Bianchet, P. Cole, A. Giaccia, and C. Wolberger for helpful discussions. This work was supported by the Johns Hopkins Institute for Cell Engineering and the Foundation for Advanced Research in the Medical Sciences. G.L.S. is the C. Michael Armstrong Professor at Johns Hopkins University School of Medicine.

1. Dewhirst MW, Cao Y, Moeller B (2008) Cycling hypoxia and free radicals regulate angiogenesis and radiotherapy response. *Nat Rev Cancer* 8:425–437.
2. Semenza GL (2003) Targeting HIF-1 for cancer therapy. *Nat Rev Cancer* 3:721–731.
3. Wang GL, et al. (1995) Hypoxia-inducible factor 1 is a basic-helix-loop-helix-PAS heterodimer regulated by cellular O_2 tension. *Proc Natl Acad Sci USA* 92:5510–5514.
4. Kaelin WG, Jr, Ratcliffe PJ (2008) Oxygen sensing by metazoans: The central role of the HIF hydroxylase pathway. *Mol Cell* 30:393–402.
5. Melillo G (2007) Targeting hypoxia cell signaling for cancer therapy. *Cancer Metastasis Rev* 26:341–352.
6. Jiang B-H, et al. (1996) Dimerization, DNA binding, and transactivation properties of hypoxia-inducible factor 1. *J Biol Chem* 271:17771–17778.
7. Paulmurugan R, Gambhir SS (2003) Monitoring protein-protein interactions using split synthetic Renilla luciferase protein-fragment-assisted complementation. *Anal Chem* 75:1584–1589.
8. Zhang H, et al. (2008) Digoxin and other cardiac glycosides inhibit HIF-1α synthesis and block tumor growth. *Proc Natl Acad Sci USA* 105:19579–19586.
9. Isaacs JS, et al. (2002) Hsp90 regulates a von Hippel-Lindau-independent hypoxia-inducible factor-1α-degradative pathway. *J Biol Chem* 277:29936–29944.
10. Gao P, et al. (2007) HIF-dependent antitumorigenic effect of antioxidants *in vivo*. *Cancer Cell* 12:230–238.
11. Du R, et al. (2008) HIF-1α induces the recruitment of bone marrow-derived vascular modulatory cells to regulate tumor angiogenesis and invasion. *Cancer Cell* 13:206–220.
12. Card PB, Erbel PJ, Gardner KH (2005) Structural basis of ARNT PAS-B dimerization: use of a common β-sheet interface for hetero- and homodimerization. *J Mol Biol* 353:664–677.
13. Scheuermann TH, et al. (2009) Artificial ligand binding within the HIF-2α PAS-B domain of the HIF2 transcription factor. *Proc Natl Acad Sci USA* 106:450–455.
14. Wainwright M (2001) Acridine—a neglected antibacterial chromophore. *J Antimicrob Chemother* 47:1–13.
15. Goldie H, Walker M, Graham T, Williams F (1959) Topical effect of acriflavine compounds on growth and spread of malignant cells. *J Natl Cancer Inst 23:841–845.*
16. Choi SH, et al. (2000) Inhibition of lipopolysaccharide-induced IκB degradation and tumor necrosis factor α expression by acriflavine, an antimicrobial agent. *Int J Immunopharmacol* 22:775–787.